17th International Drying Symposium (IDS 2010)
Magdeburg, Germany, 3-6 October 2010

ON THE MODELING OF CONVECTIVE DRYING TESTS ON SOIL SAMPLES IN NON-ISOTHERMAL CONDITIONS

P. Gerard[1], A. Léonard[2], R. Charlier[1], F. Collin[1,3]

[1]Université de Liège – Département ArGEnCo
Chemin des Chevreuils, 1 – 4000 Liège, Belgium
Tel.:+32 4 366 91 43, E-mail: pgerard@ulg.ac.be, Robert.Charlier@ulg.ac.be, f.collin@ulg.ac.be

[2]Université de Liège – Département de Chimie Appliquée
E-mail: a.leonard@ulg.ac.be

[3]FNRS Research Associate

Abstract: This paper deals with the moisture exchanges occurring in soil-atmosphere interaction problems. Convective drying tests are performed on silt samples in order to reproduce the natural drying conditions. The experimental results provide relevant data on the transfer kinetics into the boundary layer. A coupled formulation of the vapor and energy exchanges is proposed. The modeling results of the drying tests present a good agreement with the observed kinetics of the materials desaturation. Our model enables the analysis of the moisture transport mechanisms into and at the boundary of the samples.

Keywords: soil-atmosphere interaction, vapor exchange, convective drying test, modeling, partially saturated

INTRODUCTION

The modeling of unsaturated drying deformable materials is a crucial issue in civil engineering. The geomaterials, as rocks, soils or concrete, can be subjected to gradients of relative humidity or temperature.

For cement based materials, the durability issues in civil engineering have to be studied during very long periods of time over which the main causes of change in liquid water content are the interactions with ambient atmosphere (Baroghel-Mainguy et al., 2001). For soils, the problem of drought in some regions induces ground movements associated to shrink/swell of soils, particularly in clayey soils (Cui et al., 2005). This is a major cause of worry for specialists involved in the field of constructions. Ventilation in tunnels influences also the desaturation and the mechanical behavior of the host rock near the wall (Gerard et al., 2008a).

These latter examples of soil-atmosphere interactions emphasize the need of correct flow boundary conditions in order to deduce the moisture distributions into the geomaterials in interaction with the ambient atmosphere. All these problems can be related to the drying of an unsaturated porous medium, which is a process of moisture removal from materials. The study of the drying mechanisms can be performed through convective drying tests on soil samples, where the conditions (temperature, relative humidity or wind velocity) of the interactions between porous media and the ambient atmosphere are reproduced.

Owing to the variation of the drying conditions during soil-atmosphere interaction problems, evaporation at the soil surface is the result of two coupled processes occurring at the same time: vapor and heat exchanges (Olivella and Gens, 2000). Moreover, we assume that the heat and vapor exchanges with the atmosphere take place in a boundary layer at the surface of the porous medium, in addition to the heat and water flows which occur into the porous medium. Mass and energy transfers in the boundary layer are controlled by mass and heat transfer coefficients characterizing the boundary layer (Keey, 1972; Mujumdar, 1995; Perré, 1997; Perré and Turner, 1999; Coumans, 2000; Kowalski, 2003). According to the characteristics of the material and the drying conditions, either the internal transport of water or the vapor exchanges into the boundary layer becomes the limiting mechanism which controls the drying.

In this paper, a short overview of the drying processes is achieved. Different convective drying experiments are then presented for silts at different drying conditions. From a formulation of the vapor

and heat exchanges occurring at porous medium surface (Key, 1972; Coumans, 2000), mass and heat transfer coefficients characterizing the boundary layer are determined for the different drying conditions. This formulation is then introduced in the finite element code Lagamine (Collin et al., 2002) in order to model the drying experiments. The numerical simulations allow a good numerical reproduction of the kinetics of the materials desaturation observed during the drying tests. The model allows the study of the moisture transport mechanisms in the materials. Such analysis highlights the limiting mechanism controlling drying.

DRYING PROCESSES

Kinetics of drying processes

The convective drying kinetics of samples can be analyzed from the continuous weight measurement of samples. The corresponding drying rate is usually plotted as a function of the sample water content. Three drying periods can be generally observed: a preheating period, a constant drying rate period and a falling rate period (Kowalski, 2003).

The preheating period corresponds to the increase of the drying rate and the temperature at the outer boundary of the sample reaches the wet bulb temperature of the surroundings. During the constant drying rate period, the heat supplied by the surroundings is entirely used for the vaporization of the liquid water. The temperature of the dried porous medium remains constant and equal to the wet bulb temperature. The evaporation occurs in a saturated boundary layer. The vapor and the heat transfers are only influenced by the external conditions, i.e. the drying temperature, air velocity and humidy (Nadeau and Puiggali, 1995; Geankoplis, 1993). This period continues as long as the moisture transport to the surface is sufficient to maintain the drying rate. The falling rate period is characterized by a continuous increase of the dried body temperature to the temperature of the drying medium. The drying rate decreases until the end of drying, in pursuance of the decrease of the water transfers (in liquid or gaseous phases) from the sample centre to the surface.

Vapor and heat exchanges

The mass and heat transfers with the atmosphere take place in a boundary layer all around the samples (Kowalski, 2003). These coupled exchanges occur in parallel with the water and heat flows within the materials.

The vapor flow $\overline{q}$ from the materials to the surroundings is assumed proportional to the difference of the vapor density between the surroundings and the external surface of the samples (Keey, 1972; Coumans, 2000; Léonard et al., 2005; Gerard et al., 2008a). The proportionality coefficient is a mass transfer coefficient characterizing the surface transfer properties of the boundary layer. The vapor flow is expressed as:

$$\overline{q} = \alpha.\left(\rho_v^{\Gamma} - \rho_v^{a}\right) \qquad (1)$$

with ρ_v^a and ρ_v^{Γ} the vapor density respectively in the surroundings and at the boundary of the sample and α a vapor mass transfer coefficient which mainly depends on the air velocity (Geankoplis, 1993; Dracos, 1980; Ketelaars, 1992).

Evaporation at the surface depends also on thermal conditions. The heat flux $\overline{f}$ from the boundary to the surroundings is expressed as:

$$\overline{f} = L.\overline{q} - \beta.\left(T^a - T^{\Gamma}\right) \qquad (2)$$

where T^a is the temperature of the surrounding air, T^{Γ} the temperature at the boundary of the sample, β is a thermal transfer coefficient and L is the latent heat of water vaporization (=2500 $kJ.kg^{-1}$). The first term of the heat flux is the energy needed for water vaporization at the boundary. The second term denotes the convective heat flux between the atmosphere and the porous medium.

The mass and heat coefficients, which characterize the transfers into the boundary layer, will be determined through convective drying tests. Their determination is a crucial issue for the understanding and the quantification of the soil-surface interaction mechanisms.

CONVECTIVE DRYING EXPERIMENTS

Convective drying tests are performed on Awans silt, which is a representative upper soil from Belgium. More data about the geotechnical properties of the Awans silt can be found in Masekanya (2008) and Gerard et al. (2010).

Cylindrical samples of silt (14 mm high and 17 mm in diameter, for a weight about 6.5 g) are dried during 12 hours. In order to accelerate the drying process, which is quite slow, soil samples are surrounded by very dry and hot ambient air (RH≈1% - T^a=50, 60 or 70°C). Other drying experiments are nevertheless performed with surrounding air at the ambient temperature and higher relative humidity (30% and 50%). In this way, evolution of transfer coefficients with air relative humidity or drying temperature can be deduced.

Experimental device

The drying experiments are carried out in a convective rig controlled in air relative humidity, temperature and superficial velocity (Léonard et al., 2002). The cylindrical soil sample lies in the drying chamber on a supporting grid linked underneath to a precision weighting device. The sample surroundings are such that drying can occur on the whole external surface. The sample mass is recorded every 30

seconds in order to obtain the drying curves from which the external vapor and heat transfer coefficients can be determined.

Experimental results

In this study, drying shrinkage of the materials is assumed negligible, in view of the small shrinkage limit of silts. It should be also emphasized that neither cracking nor microcracking are experimentally observed on the Awans silt samples at the end of the drying experiments. Fig. 1 presents the drying curves obtained for a series of tests performed at different relative humidities of the surrounding air at a drying temperature of 50°C: 1%, 30% and 50%. The results show the good reproducibility of the experiments and the decrease of the maximal drying rate with the increase of the air relative humidity. The two experimental curves corresponding to a relative humidity of 50 % seem to evolve differently from the others. The increase of the drying rate around a water content of 0.15 can be explained by the difficulty for the vapor generator to maintain high relative humidity. Nevertheless, the determination of the transfer coefficients is possible with the knowledge of the constant drying rate.

As explained previously, during the constant drying rate period, the temperature is assumed constant and equal to the wet bulb temperature T^h characterizing the surrounding air. The boundary of the sample is considered saturated during this period (Nadeau and Puiggali, 1995). From the maximal experimental drying flow $\overline{q}_{max}$ and the equation (1), the saturated vapor transfer coefficient is determined by:

$$\alpha_0 = \frac{\overline{q}_{max}}{\left(\rho_{v,0}^{\Gamma}\left(T^h\right) - \rho_v^a\right)} = -\frac{dM}{dt}\cdot\frac{1}{A\left(\rho_{v,0}^{\Gamma}\left(T^h\right) - \rho_v^a\right)} \quad (3)$$

where $\rho_{v,0}^{\Gamma}$ is the saturated vapor density at the boundary of the sample.

The constant drying rate period clearly appears for high air relative humidity, but less for drier air. It can be explained by the fact that the drying process is slower in samples submitted to humid surrounding air than in those submitted to dry surrounding air. In the case of severe drying conditions, i.e. dry air, the internal transport of water becomes the limiting step and no constant drying rate period can be observed. Moreover, it was quite difficult to produce completely saturated samples. When experiments do not produce any constant rate period, it is rather complicated to determine the external transfer coefficient. However, as a first estimate, the maximum drying rate is considered to approach the value of the transfer coefficients from equation (3). Fig. 2 shows the decrease of the mass transfer coefficient with the air relative humidity.

The heat transfer coefficient β can also be deduced from the experimental data assuming a constant temperature in the boundary layer during the constant drying rate period equal to the wet bulb temperature. From equation (2), it comes:

$$\beta = \frac{L.\overline{q}_{max}}{T^a - T^h} \quad (4)$$

Evolution of heat transfer coefficient with the air relative humidity is not presented in this document, but can be consulted in Gerard et al. (2010).

Other drying conditions (different drying temperatures or air velocities) have been also tested, but the experimental results are not presented in this paper (see Gerard et al., 2008b; Gerard et al., 2010).

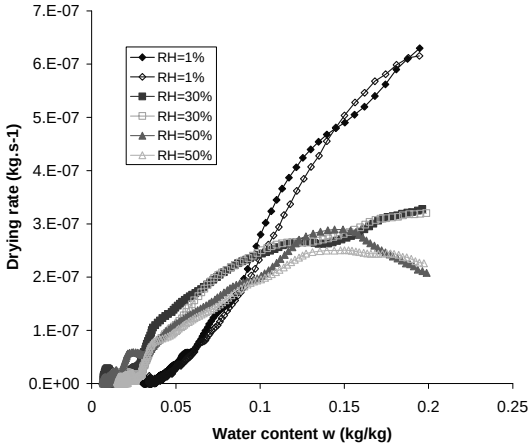

Fig. 1. Drying rate curves for different air relative humidities (air drying temperature T^a = 50°C - air velocity = 1m/s)

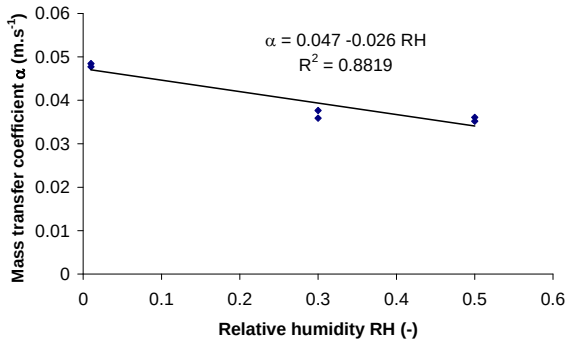

Fig. 2. Mass transfer coefficient according to air relative humidity (air drying temperature T^a = 50°C - air velocity = 1 m/s)

NUMERICAL MODELING

Boundary value problem

2D-axisymetric modeling of cylindrical samples is performed in order to compare the convective drying experimental data with the simulation results. The porous medium is assumed rigid. Gas pressure is assumed constant and equal to the atmospheric pressure.

The geometry of the problem is presented on Fig. 3. The samples are initially saturated and their initial temperature is the ambient temperature (= 17°C). Heat and flow transfers with the exterior are described by the equations (1) and (2). Mass and heat transfer coefficients computed from the drying experiments (see the previous section) are used in the boundary conditions expressions.

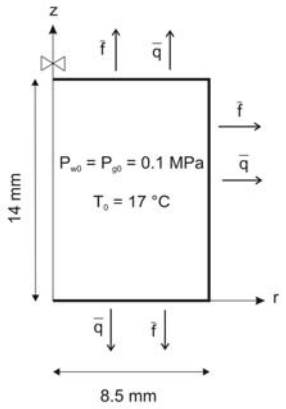

Fig. 3. Boundary value problem of drying experiment

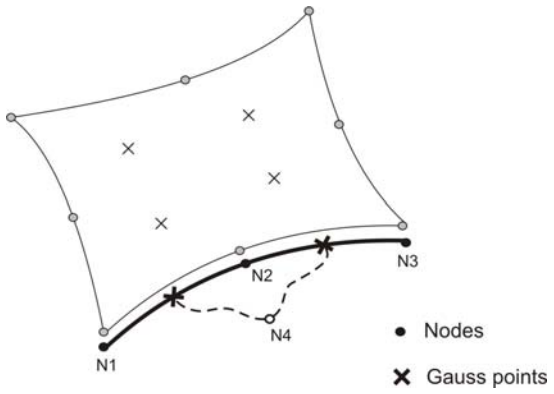

Fig. 4. Two-dimensional finite element and boundary element

To reproduce the water vapor and heat flows occurring at the sample surface, we need classical quadrilateral 2D finite elements associated with a new boundary finite element through which the hydraulic and heat exchanges between the porous medium and the surroundings take place (Gerard et al., 2008a). The special thermo-hydraulic boundary condition is defined by four nodes (Fig. 4). The first three nodes are located on the boundary (N1, N2 and N3). They allow a spatial discretization of the water pressure and temperature distribution along the boundary. The fourth node (N4) is introduced to define the relative humidity and the temperature of the surroundings (as far as they correspond to the d.o.f. of the fourth node). Its geometrical position does not influence the results. Two Gauss points are considered for the boundary finite element. The thermo-hydraulic flow is computed thanks to equations (1) and (2), where the vapor density and temperature of the surroundings is computed at the fourth node and the vapor density and temperature at the boundary of the sample is evaluated at the Gauss points. Even tough the atmosphere conditions remain constant during the drying tests this fourth node will be helpful for the modeling of soil-atmosphere interaction problems or drying experiments where the drying conditions evolve with time. More details on the numerical formulation of the boundary finite element can be found in Gerard et al. (2008a).

Hydraulic and thermal behaviors

The mass flow into the porous medium is defined by the sum of the advection of the liquid water (Darcy's law for unsaturated cases) and the diffusion of water vapor (Fick's diffusion law, as proposed by Philip and de Vries (1957)):

$$V_i = m_{i,w} + i_{i,v} = -\rho_w \frac{\kappa\, k_{r,w}}{\mu_w}\left(\frac{\partial p_w}{\partial x_i} + \rho_w g_i\right) - D\tau\phi\left(1 - S_{r,w}\right)\frac{\partial \rho_v}{\partial x_i} \quad (5)$$

where κ is the intrinsic permeability, $k_{r,w}$ is water relative permeability, μ_w is the water dynamic viscosity (=10^{-3} Pa.s), D is the molecular diffusion coefficient of the mixture of gaseous air and water vapor (=2.78 10^{-5} m².s^{-1} in STP conditions), τ the tortuosity and ρ_v the vapor density.

The advective flux of the gaseous phase is neglected, because the gas pressure remains constant. From experimental data on Awans silt and other Belgian silts (Gerard et al., 2010), a van Genuchten retention curve is adopted (van Genuchten, 1980):

$$S_{r,w} = \left[1 + \left(\frac{p_c}{P_r}\right)^{\frac{1}{1-n}}\right]^{-n} \quad \text{and } S_{r,w} = 1 \text{ if } p_c < 0 \quad (6)$$

with $S_{r,w}$ the degree of saturation, p_c the capillary pressure and P_r and m two parameters. The water relative permeability function proposed by van Genuchten (1980) is used:

$$k_{r,w} = \sqrt{S_{r,w}}\left[1 - \left(1 - S_{r,w}^{1/n}\right)^n\right]^2 \quad (7)$$

The heat transport is related to three effects: conduction, convection by the fluids and evaporation:

$$t_i = -\lambda \frac{\partial T}{\partial x_i} + \left(c_{p,w}\rho_w f_{i,w} + c_{p,v} i_{i,v}\right)\left(T - T_0\right) + L i_{i,v} \quad (8)$$

with λ the medium conductivity, $c_{p,w}$ the water specific heat (=4180 $W.m^{-1}.K^{-1}$), $c_{p,v}$ the vapor specific heat (=1000 $W.m^{-1}.K^{-1}$) and L the latent heat of water vaporization (=2500 $kJ.kg^{-1}$). The enthalpy of the system is given by the sum of each component's enthalpy:

$$h = \phi S_{r,w}\rho_w c_{p,w}\left(T - T_0\right) + \left(1-\phi\right)\rho_s c_{p,s}\left(T - T_0\right) + \phi\left(1 - S_{r,w}\right)\rho_v c_{p,v}\left(T - T_0\right) + \phi\left(1 - S_{r,w}\right)\rho_v L \quad (9)$$

with $c_{p,s}$ the solid specific heat.

All the details about the coupled thermo-hydraulic formulation can be found in Collin et al. (2002).

The hydraulic and thermal parameters of Awans silt have been determined by Masekanya (2008) and are presented in Table 1. It is known that the thermal conductivity of soils depends on temperature and saturation, but a constant thermal conductivity is used in the modeling, due to a lack of experimental data on Awans silt.

Table 1. Awans silt parameters for thermo-hydraulic model

κ	Intrinsic permeability	5 10^{-14} m²
ϕ	Porosity	0.35
τ	Tortuosity	0.10
P_r	Van Genuchten parameter	0.05 MPa
n	Van Genuchten parameter	0.26
$c_{p,s}$	Solid grains specific heat	879 J kg^{-1} K^{-1}
λ	Thermal conductivity	1.3 W m^{-1} K^{-1}

Influence of flow boundary conditions

A drying test performed with an air relative humidity of 30% and a temperature of 50°C is modeled. The advantage of this experiment is that the air relative humidity is situated in a range of values where the retention behavior is well known. In a first simulation, we assume that the boundary layer, where the vapor transfers occur, remains saturated during drying. The value of the mass transfer coefficient, as well as the heat transfer coefficient, is those determined from experimental results during the constant drying rate period.

The drying curve obtained with these parameters is presented in the Fig. 5. The constant drying rate period obtained with the modeling is more pronounced than the one observed experimentally.

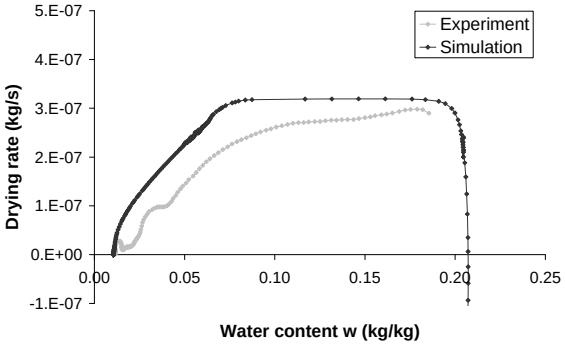

Fig. 5. Drying rate curves – Comparison between experimental and numerical results (drying tests with air RH=30% and T^a=50°C)

The overestimation of the drying rate should be related to the fact that the boundary layer where the vapor exchanges take place does not remain saturated during the falling drying rate period, due to the slowness of moisture transport comparing to the capacity of evaporation of the boundary layer. To take into account the desaturation of the boundary layer, equation 1 is modified by introducing the degree of saturation at the boundary surface:

$$\overline{q} = \alpha_0 S_{r,w}^{\Gamma}\left(\rho_v^{\Gamma} - \rho_v^a\right) \quad (10)$$

with α_0 the saturated vapor transfer coefficient, corresponding to the one determined during the constant drying rate period.

With this new flow boundary condition, numerical results present good agreement with experimental measurements, as shown in Fig. 6. Due to the desaturation of the boundary layer, the constant drying rate period is reduced and the falling rate period begins earlier.

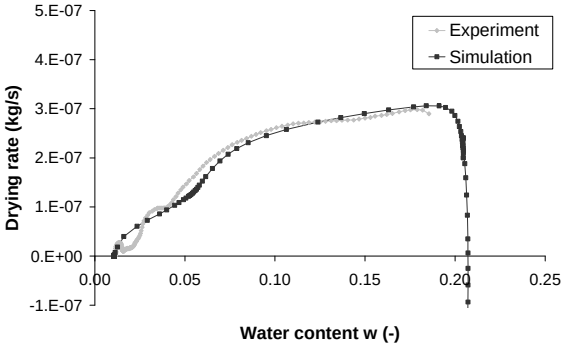

Fig. 6. Drying rate curves with new flow boundary condition – Comparison between experimental and numerical results (drying test with air RH=30% and T^a=50°C)

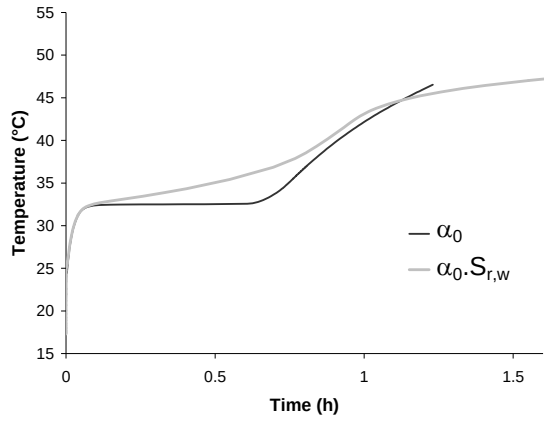

Fig. 7. Numerical time evolution of temperature at the silt surface – Comparison the two flow boundary conditions results (drying test with air RH=30% and T^a=50°C)

Moreover, on the contrary to the first case (flow boundary condition expressed in equation (1) – saturated boundary layer), the temperature at the boundary of the sample does not remain constant at the wet bulb temperature during the constant drying rate period (Fig. 7). This is due to the desaturation reducing the moisture transport to the boundary. The heat provided by the atmosphere is sufficient enough for the quantity of water evaporating at the boundary layer and, as a consequence, temperature at the boundary increases.

MOISTURE TRANSPORT MECHANISMS

The purpose of this section is the study of the moisture transport during the drying of highly permeable materials: is it mainly achieved by water evaporation within the sample followed by vapor diffusion toward the ambient medium (i.e. 1 + 2 in Fig. 8) or by the liquid water transport to the boundary of the sample where it evaporates (i.e. 1' + 2' in Fig. 8) (Mainguy et al., 2001)?

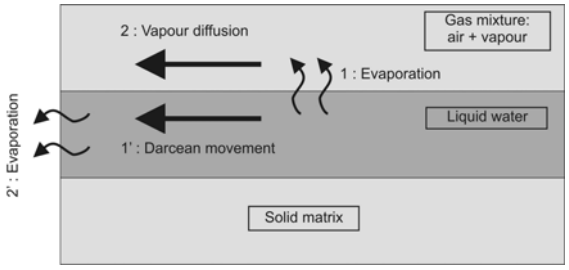

Fig. 8. Schematic representation of two extreme moisture transport mechanisms (Mainguy et al., 2001)

Fig. 10 presents the temporal evolution of water and vapor flows at the sample surface (in the middle of the height of the sample) obtained from numerical modeling of drying experiments on silt. We show that moisture is first mainly removed by liquid water advection (Darcy's law). When the desaturation of the boundary begins, Darcy's water flow decreases and vapor diffusion becomes predominant at the sample surface.

The profiles of water and vapor flows along a horizontal section situated at the middle of the height of the sample (Fig. 10) show that in a first time the transport of humidity within the whole sample corresponds in its major part to the internal transport of liquid, followed by evaporation at the sample surface. The limiting step is thus the exchanges in the boundary layer. Vapor density is uniform into the sample (Fig. 11). Due to temperature increase, intense evaporation occurs at the sample boundary and desaturation of silts begins. Water advection decreases and vapor density gradient appears in the desaturated zone. A receding front is created and moves to the heart of the sample. The limiting step becomes the internal liquid transport, as the relative permeability is decreasing. The extent of the desaturated zone increases with time. After 2h30 of drying, the vapor distribution becomes again uniform into the sample and the vapor diffusion flows decrease with time (Fig. 9, 10 and 11).

Modeling of silts drying emphasizes the influence of vapor diffusion, which was negligible with weakly permeable materials as argillaceous rock (Coussy, 2004).

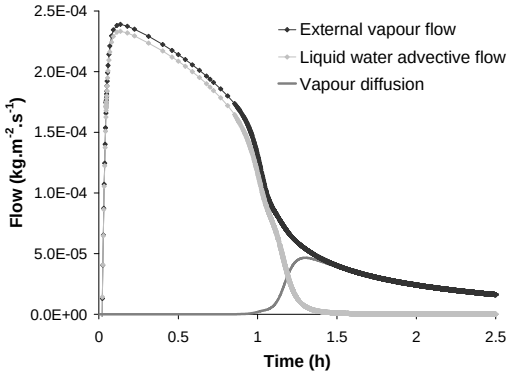

Fig. 9. Temporal evolution of water and vapor flows at the sample surface (in the first element at the middle of the height) – Drying modeling with RH=30% - T^a=50°C

CONCLUSIONS

When geomaterials are submitted to interactions with the atmosphere, the correct modeling of the coupled vapor and heat exchanges occurring at the surface is needed in order to determine the capillary pressure distributions into the porous medium. Flow and heat boundary conditions reproducing the exchanges

occurring at soil surface are therefore needed. For these reasons, convective drying experiments have been performed on samples of Awans silt (an upper soil from Belgium) under different drying conditions (air temperature and relative humidity). Assuming that the exchanges take place in a boundary layer, mass and heat transfer coefficients can be determined through the drying experiments on initially saturated samples. The results show that mass transfer coefficient decreases with air relative humidity.

Modeling of the drying tests under non-isothermal conditions has been performed. Assuming the existence of a boundary layer where the exchanges take place allows a good reproduction of the kinetics of drying observed during the experiments. However, it is necessary to take into account the desaturation of the boundary layer by introducing the saturation degree in the mass transfer boundary conditions. In this way, the overestimation of the drying rate is avoided, which is not the case when the capillary pressure at the boundary is numerically imposed to the ambient suction. Such modeling allow the validation of the proposed formulation for the coupled flow and heat exchanges occurring at soils surface in interaction with the atmosphere. Numerical results improve also the understanding of the moisture transfer mechanisms into the porous medium and the exchanges with the ambient atmosphere. It is showed that in a first time, liquid water advection is the main mechanism of water transport into the sample. Then vapor diffusion becomes predominant and it corresponds with the decrease of relative humidity into the sample. In future work, relative permeability obtained from experiments will be used instead of the van Genuchten function. To be physically relevant, the desaturation of the boundary layer will be expressed by correcting the vapour density at the boundary of the solid by the saturation degree.

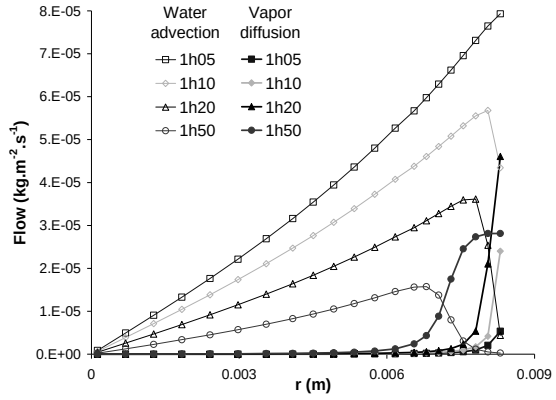

Fig. 10. Water and vapor flows profiles along horizontal section situated at the middle of the height of the sample – Drying modeling with RH=30% - T^a=50°C

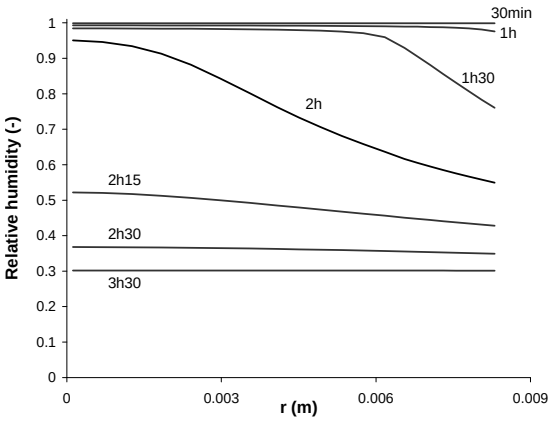

Fig. 11. Relative humidity profiles along horizontal section situated at the middle of the height of the sample – Drying modeling with RH=30% - T^a=50°C

NOMENCLATURE

A	sample area	m²
c_p	specific heat	J $kg^{-1}K^{-1}$
D	molecular diffusion	m² s^{-1}
f	heat flux at the boundary	J $m^{-2}s^{-1}$
h	enthalpy	J m^{-3}
i	diffusive mass flow	kg $m^{-2}s^{-1}$
k_r	relative permeability	-
L	latent heat of water vaporization	J kg^{-1}
n	van Genuchten parameter	-
m	advective mass flow	kg $m^{-2}s^{-1}$
M	mass	kg
p_c	capillary pressure	Pa
P_r	air entry pressure	Pa
q	vapor flow at the boundary	kg $m^{-2}s^{-1}$
S_r	degree of saturation	-
t	heat flow	J $m^{-2}s^{-1}$
T	temperature	°C
V	mass flow	kg $m^{-2}s^{-1}$

Greek letters

α	mass transfer coefficient	m s^{-1}
β	heat transfer coefficient	$Wm^{-2}kg^{-1}$
κ	intrinsic permeability	m²
λ	thermal conductivity	W $m^{-1}K^{-1}$
ϕ	porosity	-
ρ	density	kg m^{-3}
τ	tortuosity	-
μ	dynamic viscosity	Pa s

Superscripts

a	surrounding air
h	wet bulb
Γ	boundary of the sample

Subscripts

s	solid grains
v	vapor
v,0	saturated vapor
w	water

ACKNOWLEDGEMENTS

The authors would like to thank the FRS-FNRS and the European project TIMODAZ for their financial support. TIMODAZ is cofunded by the European Commission (EC) as part of the sixth Euratom research and training Framework Programme (FP6) on nuclear energy (2002– 2006).

REFERENCES

Baroghel-Mainguy, V., M. Mainguy, O. Coussy (2001), Isothermal drying process in weakly permeable cementitious materials – assesment of water permeability, Material Science of Concrete, Special Volume: Ion and Mass Transport in Cement Based Materials, Hooton RD, Thomas MDA, Marchand J, Beaudoin JJ (eds), American Ceraic Society, Westerville, pp. 59-80.

Collin, F., X.L. Li, J.-P. Radu, R. Charlier (2002), Thermo-hydro-mechanical coupling in clay barriers, Engineering Geology, Vol. 64, pp. 179-183.

Coumans, W.J. (2000), Models for drying kinetics based on drying curves of slabs, Chemical Engineering and Processing, Vol. 39(1), pp. 53-68.

Coussy, O. (2004), Poromechanics, Wiley, London.

Cui, Y.J., Y.F. Lu, P. Delage, M. Riffard (2005), Field simulation of in site water content and temperature changes due to ground-atmospheric interactions, Géotechnique, Vol. 55(7), pp. 557-567.

Dracos, Th. (1980), Hydrologie, Eine Einführung für Ingenieure, Springer-Verlag, Wien, New York.

Geankoplis, C. J. (1993), Transport processes and unit operations, Prentice-Hall, Englewood Cliffs, New Jersey.

Gerard, P., R. Charlier, R. Chambon, F. Collin (2008a), Influence of evaporation and seepage on the convergence of a ventilated cavity, Water Resources Research, Vol. 44: W00C02, doi:10.1029/2007WR006500.

Gerard, P., J Bernardino, A. Léonard, R. Charlier, F. Collin (2008b), Convective drying tests of silts: experimental study, Proceedings of the International Symposium Drought and Constructions SEC 2008, Paris, France, September 08-10 2008, pp. 149-154.

Gerard, P., A. Léonard, R. Charlier, F. Collin (2010), Study of the soil-atmosphere moisture exchanges through convective drying test in non-isothermal conditions, International Journal for Numerical and Analytical Methods in Geomechanics, doi:10.1002/nag.866.

Keey, R.B. (1972), Drying. Principles and practice, Pergamon Press, New York.

Kowalski, S.J. (2003), Thermomechanics of drying processes, Springer, Lecture Notes in Applied and Computational Mechanics.

Léonard, A., S. Blacher, P. Marchot, M. Crine (2002), Use of X-ray microtomography to follow the convective heat drying of wastewater sludges, Drying Technology, Vol. 20(4-5), pp. 1053-1069.

Léonard, A., S. Blacher, P. Marchot, J.-P. Pirard, M. Crine (2005), Convective drying of wastewater sludges: Influence of air temperature, superficial velocity and humidity on the kinetics, Drying Technology, Vol. 23(8), pp. 1667-1679.

Mainguy, M., O. Coussy, V. Baroghel-Bouny (2001), Role of air pressure in drying of weakly permeable materials, Journal of Engineering Mechanics, ASCE, Vol. 127(6), pp. 582-592.

Masekanya, J.-P. (2008), Stabilité des pentes et saturation partielle - Etude expérimentale et modélisation numérique, Ph.D. Thesis, Université de Liège.

Mujumdar, A. (1995), Handbook of industrial drying, Marcel Dekker, Inc: New-York.

Nadeau, J.-P. and J.R. Puiggali (1995), Séchage - Des processus physiques aux procédés industriels, Technique et Documentation, Lavoisier, Paris.

Olivella, S., A. Gens (2000), Vapour transport in low permeability unsaturated soils with capillary effects, Transport in Porous Media, Vol. 40, pp. 219-241.

Perré, P. (1997), Macroscopic equations to simulate heat and mass transfer. In: Mathematical modeling and numerical techniques in drying technology, Turner, I., and Mujumdar, A. S., eds.; Marcel Dekker: New York.

Perré, P and I. Turner (1999), A 3D version of Transpore : A comprehensive heat and mass transfer computational model for simulating the drying of porous media, Int. J. Heat Mass Transfer, Vol. 42(24), pp. 4501-4521.

Philip, J.R. and D.A. de Vries (1957), Moisture movement in porous materials under temperature gradients, EOS Trans. AGU, Vol. 38(2), pp. 222-232.

van Genuchten, M.Th. (1980), A closed-form equation for predicting the hydraulic conductivity of unsaturated soils, Soil Science Society of America Journal, Vol. 44, pp. 892-898.